



Universidade de São Paulo

Biblioteca Digital da Produção Intelectual - BDPI

Sem comunidade

WoS

2012

LHC discovery potential for supersymmetry with root $s=7$ TeV and $5-30 \text{ fb}^{-1}$

PHYSICAL REVIEW D, COLLEGE PK, v. 85, n. 5, supl. 1, Part 3, pp. E653-E659, 41334, 2012
<http://www.producao.usp.br/handle/BDPI/41943>

Downloaded from: Biblioteca Digital da Produção Intelectual - BDPI, Universidade de São Paulo

LHC discovery potential for supersymmetry with $\sqrt{s} = 7$ TeV and $5\text{--}30$ fb $^{-1}$ Howard Baer,^{1,*} Vernon Barger,^{2,†} Andre Lessa,^{3,‡} and Xerxes Tata^{4,§}¹*Department of Physics and Astronomy, University of Oklahoma, Norman, Oklahoma 73019, USA*²*Department of Physics, University of Wisconsin, Madison, Wisconsin 53706, USA*³*Instituto de Física, Universidade de São Paulo, São Paulo - SP, Brazil*⁴*Department of Physics and Astronomy, University of Hawaii, Honolulu, Hawaii 96822, USA*

(Received 21 December 2011; published 13 March 2012)

We extend our earlier results delineating the supersymmetry reach of the CERN Large Hadron Collider operating at a center-of-mass energy $\sqrt{s} = 7$ TeV to integrated luminosities in the range $5\text{--}30$ fb $^{-1}$. Our results are presented within the paradigm minimal supergravity model or constrained minimal supersymmetric standard model. Using a six-dimensional grid of cuts for the optimization of signal to background ratio—including missing E_T —we find for $m_{\tilde{g}} \sim m_{\tilde{q}}$ an LHC 5σ supersymmetry discovery reach of $m_{\tilde{g}} \sim 1.3, 1.4, 1.5,$ and 1.6 TeV for $5, 10, 20,$ and 30 fb $^{-1}$, respectively. For $m_{\tilde{q}} \gg m_{\tilde{g}}$, the corresponding reach is instead $m_{\tilde{g}} \sim 0.8, 0.9, 1.0,$ and 1.05 TeV, for the same integrated luminosities.

DOI: [10.1103/PhysRevD.85.051701](https://doi.org/10.1103/PhysRevD.85.051701)

PACS numbers: 14.80.Ly, 12.60.Jv, 13.85.Qk

I. INTRODUCTION

In 2011, the CERN Large Hadron Collider produced proton-proton collisions at a center-of-mass energy $\sqrt{s} = 7$ TeV (LHC7) and enabled both ATLAS and CMS experiments to each accumulate over 5 fb $^{-1}$ of useful data. The current plan is to resume running with pp collisions in early 2012, with a goal to amass in the vicinity of $10\text{--}30$ fb $^{-1}$ of usable data. The 2012 run will likely be followed by a shut down for ~ 2.5 years so that various upgrades may be implemented; a turn-on at or near design energy of $\sqrt{s} = 14$ TeV is then expected around 2015.

While many LHC analyses are focused on the elusive Higgs boson, the search for weak scale supersymmetry (SUSY) [1] remains an important part of the LHC program. In a previous paper [2], we presented projections for the LHC7 5σ discovery reach for SUSY in the paradigm minimal supergravity (mSUGRA) or constrained minimal supersymmetric standard model (CMSSM) model [3]. In that study, we presented discovery strategies for early SUSY discovery and made projections for the LHC7 reach for a variety of integrated luminosities ranging from 100 pb $^{-1}$ up to 2 fb $^{-1}$, well beyond what was then expected to be delivered in the entire 7 TeV run. LHC reach projections for $\sqrt{s} = 14$ TeV (LHC14) have been reported in earlier studies [4].

Recent analyses (performed within the mSUGRA model) of the LHC7 data by the ATLAS [5] and CMS [6] experiments based on just ~ 1 fb $^{-1}$ of integrated luminosity have found no indication of SUSY so far, yielding 95% C.L. lower limits of $m_{\tilde{q}} \sim m_{\tilde{g}} \gtrsim 1$ TeV for comparable gluino and squark masses, and $m_{\tilde{g}} \gtrsim 0.6$ TeV for the

case where $m_{\tilde{q}} \gg m_{\tilde{g}}$. It is worth emphasizing that although all squarks are by assumption degenerate within the mSUGRA framework, the squark mass limit cited above arises mostly from signals for first-generation squarks that are much more copiously produced from qq and qg initial states than their second- and third-generation cousins. In other words, the LHC7 squark limit really applies to up- and down-type squarks—other squark flavors may be significantly lighter than the quoted bounds. These LHC7 bounds do not apply to third-generation squarks or to electroweak-inos, the only sparticles with significant couplings to the Higgs sector and to which the naturalness arguments that yield upper-mass bounds on sparticles apply. Indeed, models with $\mathcal{O}(10\text{--}100)$ TeV gluinos and first-generation sfermions but with sub-TeV third-generation sfermions and electroweak-inos [7] that have been proposed to ameliorate the SUSY flavor and CP problems are not in conflict with these LHC7 data.

The LHC has performed spectacularly and has already delivered an integrated luminosity of 5 fb $^{-1}$ and, as we mentioned, is expected to deliver a comparable or larger data set in 2012. This motivated us to extend our earlier projections [2] of the LHC7 reach for SUSY to integrated luminosities up to 30 fb $^{-1}$. As before, we work within the mSUGRA framework, the parameter space of which is given by

$$m_0, \quad m_{1/2}, \quad A_0, \quad \tan\beta, \quad \text{sign}(\mu). \quad (1.1)$$

Here, m_0 is a common grand unified theory (GUT)-scale soft SUSY-breaking (SSB) scalar mass; $m_{1/2}$ is a common GUT-scale SSB gaugino mass; A_0 is a common GUT-scale trilinear SSB term; $\tan\beta$ is the ratio of the Higgs field vacuum expectation value, and μ is the superpotential Higgsino mass term whose magnitude but not sign is constrained by the electroweak symmetry-breaking minimization conditions.

*baer@nhn.ou.edu

†barger@pheno.wisc.edu

‡lessa@fma.if.usp.br

§tata@phys.hawaii.edu

For each model parameter space point, many simulated collider events are generated and compared against standard model (SM) backgrounds with the same experimental signature [8]. A six-dimensional grid of cuts [2] is then employed to enhance the SUSY signal over SM backgrounds, and the signal is deemed observable if it satisfies preselected criteria for observability. Based on previous studies [4], we include in our analysis the following channels:

- (i) jets + E_T^{miss} (no isolated leptons),
- (ii) 1ℓ + jets + E_T^{miss} ,
- (iii) two opposite-sign (OS) isolated leptons (OS) + jets + E_T^{miss} ,
- (iv) two same-sign (SS) isolated leptons (SS) + jets + E_T^{miss} ,
- (v) 3ℓ + jets + E_T^{miss} .

For the simulation of the background events, we used ALPGEN [9] to compute the hard scattering events and PYTHIA [10] for the subsequent showering and hadronization. For the final states containing multiple jets [namely, $Z(\rightarrow ll, \nu\nu)$ + jets, $W(\rightarrow l\nu)$ + jets, $b\bar{b}$ + jets, $t\bar{t}$ + jets, $Z + b\bar{b}$ + jets, $Z + t\bar{t}$ + jets, $W + b\bar{b}$ + jets, $W + t\bar{t}$ + jets, and QCD], we used the Michelangelo L. Mangano (MLM)-matching algorithm to avoid double counting. All the processes included in our analysis are shown in Table 1 of Ref. [2], as well as their total cross sections, number of events generated, and event generator used. Here, we show in Table I the various backgrounds along with k factors¹ used to normalize the generator cross sections to next-to-leading-order (NLO) QCD results where available. The background k factors were computed using MCFM [11] for the NLO cross sections and ALPGEN for the LO ones.

The signal events were generated using ISAJET 7.79 [12] which, given a mSUGRA parameter set, generates all

$2 \rightarrow 2$ SUSY processes in the right proportion and decays the sparticles to lighter sparticles using the appropriate branching ratios and decay matrix elements, until the parent sparticle cascade decay [13] terminates in the stable lightest supersymmetric particle (LSP), assumed here to be the lightest neutralino. Total gluino and squark-production cross sections have been presented in Ref. [2] at NLO QCD using PROSPINO [14] and will not be repeated here. It is worth noting that for $m_{\tilde{q}} \sim m_{\tilde{g}}$, $\tilde{g}\tilde{q}$ -associated production is the dominant, strongly interacting SUSY production mechanism, while for $m_{\tilde{q}} \gg m_{\tilde{g}}$, $\tilde{g}\tilde{g}$ -pair production tends to dominate.

For event generation, we used a toy detector simulation with calorimeter cell size $\Delta\eta \times \Delta\phi = 0.05 \times 0.05$ and $-5 < \eta < 5$. The hadronic calorimetry energy resolution is taken to be $80\%/\sqrt{E} \oplus 3\%$ for $|\eta| < 2.6$ and forward calorimetry is $100\%/\sqrt{E} \oplus 5\%$ for $|\eta| > 2.6$, where \oplus denotes a combination in quadrature. The electromagnetic calorimetry energy resolution is assumed to be $3\%/\sqrt{E} \oplus 0.5\%$. We used the cone-type ISAJET [12] jet-finding algorithm to group the hadronic final states into jets. Jets and isolated lepton are defined as follows:

- (i) Jets are hadronic clusters with $|\eta| < 3.0$, $R \equiv \sqrt{\Delta\eta^2 + \Delta\phi^2} \leq 0.4$, and $E_T(\text{jet}) > 50$ GeV.
- (ii) Electrons and muons are considered isolated if they have $|\eta| < 2.0$, $p_T(l) > 10$ GeV with visible activity within a cone of $\Delta R < 0.2$ about the lepton direction, $\sum E_T^{\text{cells}} < 5$ GeV.
- (iii) We identify hadronic clusters as b jets if they contain a B hadron with $E_T(B) > 15$ GeV, $\eta(B) < 3$, and $\Delta R(B, \text{jet}) < 0.5$. We assume a tagging efficiency of 60%, and light quark and gluon jets can be mistagged as a b jet with a probability $1/150$ for $E_T \leq 100$ GeV and $1/50$ for $E_T \geq 250$ GeV, with a linear interpolation for $100 \text{ GeV} \leq E_T \leq 250 \text{ GeV}$ [15].

As in Ref. [2], we define the signal to be observable if

$$S \geq \max[5\sqrt{B}, 5, 0.2B],$$

where S and B are the expected number of signal and background events, respectively, for an assumed value of integrated luminosity. The requirement $S \geq 0.2B$ is imposed to avoid the possibility that a *small* signal on top of a *large* background could otherwise be regarded as statistically significant, but whose viability would require the background level to be known with exquisite precision in order to establish a discovery. For cases with very low signal and background event numbers, we require the Poisson probability to correspond to the 5σ level.

¹By k factor, here, we actually mean $\sigma^{\text{NLO}}/\sigma^{\text{LO}}$. Normally, one compares the two cross sections using an identical renormalization/factorization scale for the two cases. Here, we merely compute σ^{LO} using ALPGEN and σ^{NLO} using MCFM, using the preprogrammed default scale choices for the latter.

TABLE I. Background processes included in this LHC7 study, along with the k factor [from MCFM and ALPGEN] used, when available, to normalize to NLO QCD. For $t\bar{t}$ production, the renormalization scale is chosen to match the NLO cross section. The event generator used, total cross sections, and number of generated events are listed in Table 1 of Ref. [2]. All light (and b) partons in the final state are required to have $E_T > 40$ GeV. For QCD, we generate the hardest final parton jet in distinct bins to get a better statistical representation of hard events.

SM process	k factor	SM process	k factor
$t\bar{t}$	0.99	QCD, $b\bar{b}$...
Z/γ + jets	1.47	$Z + t\bar{t}$...
W + jets	1.53	$W + t\bar{t}$...
$Z(\rightarrow \nu\bar{\nu}) + b\bar{b}$	1.18	$W + b\bar{b}$...
$Z/\gamma(\rightarrow l\bar{l}) + b\bar{b}$	1.03	$W + tb$...
WW	1.38	$t\bar{t}t\bar{t}$...
WZ	1.47	$t\bar{t}b\bar{b}$...
ZZ	1.35	$b\bar{b}b\bar{b}$...

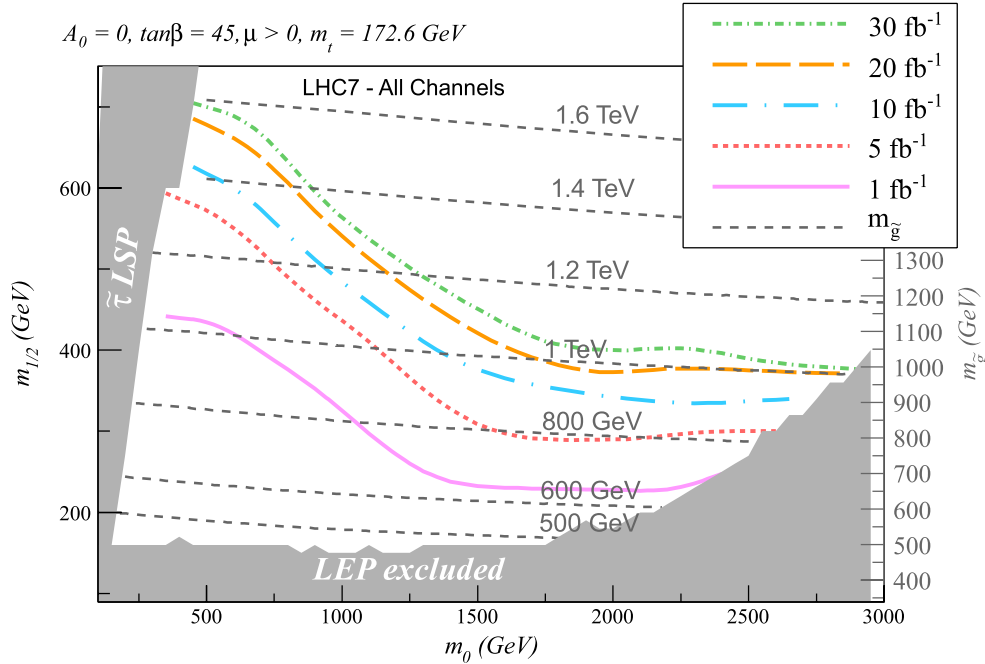


FIG. 1 (color online). The optimized SUSY reach of LHC7 for different integrated luminosities combining the different channels described in the text. The signal is observable if it falls below the solid contour for the corresponding integrated luminosity. The fixed mSUGRA parameters are $A_0 = 0$, $\tan\beta = 45$, and $\mu > 0$. Gluino mass contours are shown by the dashed, grey curves. The shaded grey area is excluded due to stau LSPs (left-side of figure) or no electroweak symmetry breaking (right-side of figure), while the shaded grey area marked “LEP excluded” is excluded by nonobservation of a sparticle signal from LEP2 searches. All sparticle and background cross sections are normalized to NLO QCD values via k factors.

The grid of cuts used in our optimized analysis is

- (i) $E_T^{\text{miss}} > 50, 100\text{--}1000$ GeV (in steps of 100 GeV);
- (ii) $n(\text{jets}) \geq 2, 3, 4, 5, \text{ or } 6$;
- (iii) $n(b\text{--jets}) \geq 0, 1, 2, \text{ or } 3$;
- (iv) $E_T(j_1) > 50\text{--}300$ GeV (in steps of 50 GeV) and $400\text{--}1000$ GeV (in steps of 100 GeV) [jets are ordered $j_1 - j_n$, from highest to lowest E_T];
- (v) $E_T(j_2) > 50\text{--}200$ GeV (in steps of 30 GeV) and $300, 400, 500$ GeV;
- (vi) $n(\ell) = 0, 1, 2, 3, (\text{OS}), (\text{SS}),$ and inclusive channel $n(\ell) \geq 0$ (here, $\ell = e, \mu$);
- (vii) $10 \text{ GeV} \leq m(\ell^+\ell^-) \leq 75 \text{ GeV}$ or $m(\ell^+\ell^-) \geq 105 \text{ GeV}$ [for the OS, same flavor dileptons only], and
- (viii) transverse sphericity $S_T > 0.2$.

We show in Fig. 1 the optimized 5σ discovery reach of LHC7 for various choices of integrated luminosity in the m_0 vs $m_{1/2}$ plane. We also take $A_0 = 0$, $\tan\beta = 45$, and $\mu > 0$, with $m_t = 172.6$ GeV.² Gluino iso-mass contours

²Recent evidence from ATLAS [17] and CMS [18] using 5 fb^{-1} of data show some evidence for a Higgs scalar h with $m_h \sim 125$ GeV. For $A_0 = 0$, it is very difficult to accommodate such a Higgs mass in the mSUGRA model. For $A_0 \sim \pm 2m_0$, then $m_h \sim 125$ GeV can be accommodated but mainly at rather high $m_0 \sim 2\text{--}10$ TeV. For more details, see e.g. Ref. [19]. Our reach projections are largely insensitive to variation in A_0 (and subsequent small changes in m_h) as explained below.

are shown as obtained using the ISASUGRA routines [16] in ISAJET. We see from Fig. 1 that with $\sim 1 \text{ fb}^{-1}$ of integrated luminosity, the LHC7 sensitivity does indeed extend to $m_{\tilde{g}} \sim 1.1$ TeV for $m_{\tilde{q}} \sim m_{\tilde{g}}$ and to $m_{\tilde{g}} \sim 0.65$ TeV for $m_{\tilde{q}} \gg m_{\tilde{g}}$.³ For 5 fb^{-1} of integrated luminosity [for which we expect ATLAS and CMS analyses in spring 2012], the LHC discovery reach extends to $m_{\tilde{g}} \sim 1.3$ TeV for $m_{\tilde{q}} \sim m_{\tilde{g}}$ and to $m_{\tilde{g}} \sim 0.8$ TeV for $m_{\tilde{q}} \gg m_{\tilde{g}}$. As integrated luminosity moves into the $20\text{--}30 \text{ fb}^{-1}$ regime, the LHC7 reach for $m_{\tilde{q}} \sim m_{\tilde{g}}$ moves up to $m_{\tilde{g}} \sim 1.5\text{--}1.6$ TeV. For the case where $m_{\tilde{q}} \gg m_{\tilde{g}}$, the $20\text{--}30 \text{ fb}^{-1}$ LHC reach approaches $m_{\tilde{g}} \sim 1$ TeV. We stress that—as discussed above—while nonobservation of the signal at LHC7 may qualitatively point toward very heavy gluinos and first-generation squarks, *this does not* in and of itself preclude SUSY as the new physics that stabilizes the weak scale [7] because third-generation squarks and electroweak-inos could still be at the sub-TeV scale.

While our results are presented for the particular choice of mSUGRA parameters $A_0 = 0$ and $\tan\beta = 45$, we emphasize here that we expect these results to also hold for

³We stress that the curves presented here include an optimization over several search channels and correspond to a 5σ discovery reach. Care must be taken when comparing these results with experimental bounds, which are usually presented for single channels at 95% C.L. ($\sim 2\sigma$).

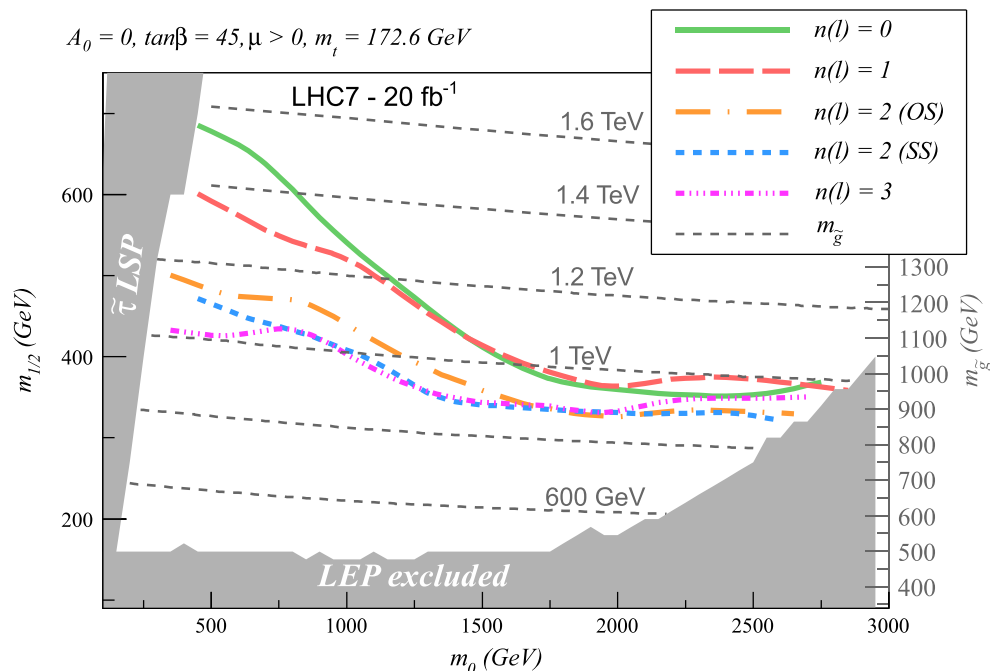


FIG. 2 (color online). The optimized 5σ SUSY reach of LHC7 in various channels classified by lepton multiplicity: 0ℓ , 1ℓ , SS dilepton, OS dilepton and trilepton for an integrated luminosity of 20 fb^{-1} . Any mSUGRA point will be observable if it falls below the corresponding contour. The fixed mSUGRA parameters are $A_0 = 0$, $\tan\beta = 45$, and $\mu > 0$. Gluino mass contours are shown by the dashed, grey curves. The shaded grey area is excluded due to tau LSPs (left-side of figure) or no electroweak symmetry breaking (right-side of figure), while the shaded grey area marked “LEP excluded” is excluded by nonobservation of a sparticle signal from LEP2 searches. All sparticle and background cross sections are normalized to NLO QCD values via k factors.

other choices of A_0 and $\tan\beta$ and also for $\mu < 0$. Variation of A_0 mainly affects third-generation sparticle masses, while the reach is determined mostly by $m_{\tilde{g}}$ and the first-generation squark masses. Moreover, variation of $\tan\beta$ mainly affects the size of b and τ Yukawa couplings, and these feed only weakly into the reach plots: for instance, sparticle decays to third-generation matter are enhanced at large $\tan\beta$ [20] where b -tagging may somewhat enhance the LHC reach for gluinos [21], as already demonstrated by ATLAS [22].

To give the reader an idea of the dominant event topologies in which experiments at LHC7 will be able to probe SUSY in the 2012 run, we show in Fig. 2 the optimized 5σ reach via the 0ℓ , 1ℓ , OS dilepton, SS dilepton, and the trilepton channels for 20 fb^{-1} . The striking feature of the figure is that while the reach is dominated by the low-multiplicity ($n_\ell = 0, 1$) lepton channels for $m_0 \lesssim 1.5 \text{ TeV}$, the reach in the low-background but rate-limited trilepton channel becomes competitive with that in other channels if squarks are essentially decoupled at LHC7, as

could well be the case. We have checked that this is also true for an integrated luminosity of 10 fb^{-1} .

In summary, we have presented updated 5σ discovery contours for the paradigm mSUGRA/CMSSM SUSY model for LHC7 with $5\text{--}30 \text{ fb}^{-1}$ of integrated luminosity. These results help us to understand the capabilities of LHC7 for discovering supersymmetry in 2012–2013. Within mSUGRA, for integrated luminosity $20\text{--}30 \text{ fb}^{-1}$, we expect LHC7 to probe $m_{\tilde{g}}$ up to $\sim 1.6 \text{ TeV}$ for $m_{\tilde{q}} \approx m_{\tilde{g}}$, while we expect LHC7 to probe up to $m_{\tilde{g}} \sim 1 \text{ TeV}$ for $m_{\tilde{q}} \gg m_{\tilde{g}}$. If squarks are much heavier than gluinos, the reach at LHC7 via the inclusive trilepton channel will be competitive in reach with the canonical jets plus E_T^{miss} channel.

ACKNOWLEDGMENTS

This work was supported by the United States Department of Energy and by Fundação de Apoio à Pesquisa do Estado de São Paulo (FAPESP).

- [1] The minimal supersymmetric standard model commonly used today was introduced by S. Dimopoulos and H. Georgi, *Nucl. Phys.* **B193**, 150 (1981); N. Sakai, *Z. Phys.* **C 11**, 153 (1981); for reviews of SUSY phenomenology, see H. Baer and X. Tata, *Weak Scale Supersymmetry: From Superfields to Scattering Events* (Cambridge University Press, Cambridge, England 2006); M. Drees, R. Godbole, and P. Roy, *Theory and Phenomenology of Sparticles* (World Scientific, Singapore, 2004); P. Binetruy, *Supersymmetry* (Oxford University Press, New York, 2006); S.P. Martin, in *Perspectives on Supersymmetry II*, edited by G.L. Kane (World Scientific, Singapore, 2010), Chap. 1, p. 153.
- [2] H. Baer, V. Barger, A. Lessa, and X. Tata, *J. High Energy Phys.* **06** (2010) 102.
- [3] A. Chamseddine, R. Arnowitt, and P. Nath, *Phys. Rev. Lett.* **49**, 970 (1982); R. Barbieri, S. Ferrara, and C. Savoy, *Phys. Lett.* **119B**, 343 (1982); N. Ohta, *Prog. Theor. Phys.* **70**, 542 (1983); L. Hall, J. Lykken, and S. Weinberg, *Phys. Rev. D* **27**, 2359 (1983).
- [4] H. Baer, X. Tata, and J. Woodside, *Phys. Rev. D* **45**, 142 (1992); H. Baer, C. H. Chen, F. Paige, and X. Tata, *Phys. Rev. D* **52**, 2746 (1995); **53**, 6241 (1996); H. Baer, C. H. Chen, M. Drees, F. Paige, and X. Tata, *Phys. Rev. D* **59**, 055014 (1999); H. Baer, C. Balázs, A. Belyaev, T. Krupovnickas, and X. Tata, *J. High Energy Phys.* **06** (2003) 054; See also, S. Abdullin and F. Charles, *Nucl. Phys.* **B547**, 60 (1999); S. Abdullin *et al.* (CMS Collaboration), *J. Phys. G* **28**, 469 (2002); B. Allanach, J. Hetherington, A. Parker, and B. Webber, *J. High Energy Phys.* **08** (2000) 017; H. Baer, V. Barger, A. Lessa, and X. Tata, *J. High Energy Phys.* **09** (2009) 063; E. Izaguirre, M. Manhart, and J. Wacker, *J. High Energy Phys.* **12** (2010) 030.
- [5] G. Aad *et al.* (ATLAS Collaboration), [arXiv:1109.6572](https://arxiv.org/abs/1109.6572).
- [6] S. Chatrchyan *et al.* (CMS Collaboration), *Phys. Rev. Lett.* **107**, 221804 (2011).
- [7] M. Dine, A. Kagan, and S. Samuel, *Phys. Lett. B* **243**, 250 (1990); N. Arkani-Hamed and H. Murayama, *Phys. Rev. D* **56**, R6733 (1997); S. Dimopoulos and G. Giudice, *Phys. Lett. B* **357**, 573 (1995); A. Pomarol and D. Tomassini, *Nucl. Phys.* **B466**, 3 (1996); A. Cohen, D. B. Kaplan, and A. Nelson, *Phys. Lett. B* **388**, 588 (1996); H. Baer, S. Kraml, A. Lessa, S. Sekmen, and X. Tata, *J. High Energy Phys.* **10** (2010) 018; H. Baer, V. Barger, and P. Huang, *J. High Energy Phys.* **11** (2011) 031.
- [8] For perspective on SM background to SUSY signals, see e.g. H. Baer, V. Barger, and G. Shaughnessy, *Phys. Rev. D* **78**, 095009 (2008); M. Mangano, and (CERN Collaboration) *Eur. Phys. J. C* **59**, 373 (2009); H. Baer, [arXiv:0901.4732](https://arxiv.org/abs/0901.4732).
- [9] M. Mangano, M. Moretti, F. Piccinini, R. Pittau, and A. Polosa, *J. High Energy Phys.* **07** (2003) 001.
- [10] T. Sjostrand, S. Mrenna, and P. Skands, *J. High Energy Phys.* **05** (2006) 026.
- [11] J. Campbell and R.K. Ellis, computer code MCFM, see R.K. Ellis *Nucl. Phys. B, Proc. Suppl.* **160**, 170 (2006).
- [12] H. Baer, F. Paige, S. Protopopescu, and X. Tata (ISAJET), [arXiv:hep-ph/0312045](https://arxiv.org/abs/hep-ph/0312045).
- [13] H. Baer, J. R. Ellis, G. B. Gelmini, D. V. Nanopoulos, and X. Tata (CERN Collaboration), *Phys. Lett.* **161B**, 175 (1985); G. Gamberini, *Z. Phys. C* **30**, 605 (1986); H. Baer, V. Barger, D. Karatas, and X. Tata, *Phys. Rev. D* **36**, 96 (1987); H. Baer, X. Tata, and J. Woodside, *Phys. Rev. D* **45**, 142 (1992).
- [14] W. Beenakker, R. Hopker, and M. Spira, [arXiv:hep-ph/9611232](https://arxiv.org/abs/hep-ph/9611232).
- [15] S. Corréad, V. Kostoukhine, J. Levêque, A. Rozanov, and J. B. de Vivie, ATLAS Report No. ATLAS-PHYS-2004-006 2004; V. Kostoukhine, ATLAS Report No. ATLAS-PHYS-2003-033 2003.
- [16] H. Baer, C. H. Chen, R. Munroe, F. Paige, and X. Tata, *Phys. Rev. D* **51**, 1046 (1995); H. Baer, J. Ferrandis, S. Kraml, and W. Porod, *Phys. Rev. D* **73**, 015010 (2006).
- [17] F. Gianotti (ATLAS Collaboration), CERN, Report No. ATLAS-CONF-2011-163, 2011.
- [18] G. Tonelli (CMS Collaboration), CERN, 2011 (unpublished).
- [19] H. Baer, V. Barger, and A. Mustafayev, [arXiv:1112.3017](https://arxiv.org/abs/1112.3017).
- [20] H. Baer, C.-h. Chen, M. Drees, F. Paige, and X. Tata, *Phys. Rev. Lett.* **79**, 986 (1997); *Phys. Rev. D* **59**, 055014 (1999).
- [21] U. Chattopadhyay, A. Datta, A. Datta, A. Datta, and D. P. Roy, *Phys. Lett. B* **493**, 127 (2000); P. G. Mercadante, J. K. Mizukoshi, and X. Tata, *Phys. Rev. D* **72**, 035009 (2005); S. P. Das, A. Datta, M. Guchait, M. Maity, and S. Mukherji, *Eur. Phys. J. C* **54**, 645 (2008); R. Kadala, P. G. Mercadante, J. K. Mizukoshi, and X. Tata, *Eur. Phys. J. C* **56**, 511 (2008).
- [22] G. Aad *et al.* (ATLAS Collaboration), *Phys. Lett. B* **701**, 398 (2011).